Microencapsulation in Polyurea Shell: Kinetics and Film Structure

S. K. Yadav, Kartic C. Khilar, and A. K. Suresh
Dept. of Chemical Engineering, Indian Institute of Technology, Bombay 400 076, India

Interfacial polycondensation is an important polymerization technique that encapsulates a variety of active principles. Mechanisms governing the reaction and interplay of physical and chemical rate processes need to be understood for both rational design of reaction equipment and the process control to produce capsules with desired characteristics. A theoretical and experimental study of the process is reported here. Kinetic data were obtained over a range of concentrations, monomer mole ratios and polymer film thicknesses, using a technique that relies on the on-line measurement of pH as a function of time. To understand the mechanisms the reaction was slowed down by reducing the interfacial area. A minimum thickness of the polymer was observed to be necessary so that capsules preserve their integrity and do not break up. The theoretical model developed considers ionic equilibria in the aqueous phase and the resistances due to external mass transfer, diffusion through the polymer, and interfacial reaction. Under the conditions chosen, the resistance due to the chemical reaction is generally more dominant. Values of rate parameters were determined by fitting the model to the experimental data. Observed variations in the diffusivity between different experiments were rationalized through a study of the crystalline structure of polymers.

Introduction

Microencapsulation of active principles such as drugs, pesticides and herbicides is finding applications in diverse fields. For example, applications in controlled release technology (Koestler, 1980; Beestman and Deming, 1983), artificial cells, and enzyme immobilization (Chang, 1964) have been reported. Interfacial polycondensation (Morgan, 1965) is a convenient technique for carrying out such microencapsulation. Interfacial polycondensation is also of importance in its own right, as it offers the possibility of rapid production of polymers with high and specific molecular weight ranges under mild conditions of temperature and pressure.

Whether for microencapsulation or for polymer synthesis, it is usual to carry out the interfacial polycondensation reaction by bringing the reactants, dissolved in mutually immiscible phases, into contact by dispersing one phase as fine drops in the other. Apart from the usual transport resistances in such heterogeneous systems, the formation of the insoluble polymer film brings about an additional resistance in this case. The need for a fundamental understanding of the interplay between the physical and chemical rate processes in such cases is well recognized in the literature on heterogeneous reactions. In the case of a polymerization reaction, the rate processes involved could also influence such important properties of the polymer as its molecular weight, degree of crystallinity, etc., and hence, the functional properties of the polymer. An understanding of kinetic features would therefore help in deciding appropriate preparation conditions, depending on the properties desired in the product.

In this work, a comprehensive theoretical and experimental study is undertaken of the kinetics of the interfacial polycondensation reaction leading to the formation of polyurea microcapsules. Further, the structure of the polymer has been studied through X-Ray diffraction (XRD). The results provide clues on how the structure can be manipulated through the rate of polymerization.

Scope of Present Work

Interfacial polycondensation emerged as a technique of importance in the 1950s and the early work is well described

Correspondence concerning this article should be addressed to A. K. Suresh.

by Morgan (1965). Among the more significant features of interfacial polycondensation are the extremely high reaction rates (even under ambient conditions), and the high molecular weights achieved (even under conditions deviating from stoichiometric equivalence of the monomers). The distribution of molecular weights and the relative insensitivity of the average molecular weight to the monomer mole ratio point to significant differences in the kinetic mechanisms from the case of homogeneous polycondensations.

Notwithstanding the name, the locale of the reaction has been a matter of debate. Morgan (1965) suggested that the reaction is almost always on the *organic side* of the interface, but MacRitchie (1968) concluded that the polymerization occurs in a *mixed monolayer of adsorbed monomers*. Again, Kondo (1978) cited the observed influence of the partition coefficient of the aqueous-phase monomer between the two phases as evidence that the reaction occurs close to, but not at, the interface.

There have been only a few systematic studies on the kinetics of interfacial polycondensation systems, particularly in cases where the polymer precipitates out and forms a film. Most of the available literature is on polyamides. It is known that the reaction is very fast, and most likely becomes diffusion limited in most situations (Morgan, 1965; Chai and Krantz, 1994). For example, the rate of formation of nylon in an unstirred system depends on the rate of polymer withdrawal, and the reaction essentially ceases once a certain thickness of the film is produced. Most earlier studies (Pearson and Williams, 1985; Sirdesai and Khilar, 1988; Yadav et al., 1990) have modeled the reaction as involving diffusion of one of the monomers through the polymer film and reaction at the inner boundary of the film. The model of Yadav et al. (1990) provides quantitative criteria for discerning the rate of controlling phenomenon. Yadav et al. (1990) also conducted experiments on the encapsulation of Butachlor, a herbicide, in polyurea, and concluded that the process was kinetically controlled under the conditions employed. They based this conclusion on the observed dependence of the encapsulation time on the average particle size. Janssen and Nijenhuis (1992) studied the encapsulation of dibutylphthalate DBP by interfacial reaction of terephthaloyldichloride TDC and diethylenetriamine DETA. They reported that during the growth of the wall, the polymer layer acts as a membrane, with a dense top-layer and a porous sublayer. The membrane, which was produced in the organic phase, was swollen by the aqueous phase. The authors concluded from light transmission microscopy studies that small drops of the aqueous phase form at the organic side of the membrane and that polymerization proceeds at the surface of such drops leading to the formation of porosity. This striking behavior does not seem to have been reported elsewhere. The phenomenon was not observed when a bifunctional amine such as hexamethylene-diamine (HMDA) or ethylenediamine (EDA) was introduced in addition to, or instead of, DETA in the aqueous phase.

Experimentally, the extremely high velocity of the reaction presents difficulties in kinetic measurements. Recently, Chai and Krantz (1994) have used two novel techniques, viz., light-reflectometry and pendant drop tensiometry in their studies on formation of polyamide membranes in an unstirred system. While the techniques provide qualitative information on the progress of the reaction, the measurements are difficult to interpret quantitatively. In the unstirred system, Chai and Krantz (1994) concluded from their measurements that the reaction becomes limited by diffusion in the organic layer or by diffusion through the polymer film, depending on the concentrations of the two monomers used. Measurements are even more difficult in the stirred systems employed in microencapsulation. Liquid phase mass transfer is likely to be fast in these systems and, therefore, conclusions from unstirred systems cannot be extended easily. The most convenient way to monitor the reaction in such cases is to choose the conditions such that the concentration of the continuous-phase monomer varies over a reasonable range, and to monitor this variation using a continuous measurement technique. Thus, Yadav et al. (1990) exploited the fact that their aqueous-phase monomer, hexamethylene diamine, was alkaline in nature and used the pH of the aqueous phase as a measure of the monomer concentration. In such a case, although the conditions for kinetic measurements have to be chosen with the possibility and accuracy of measurements in mind, the findings can be extended to other situations with the aid of a kinetic model. In general, however, the paucity of experimental data, particularly in the low conversion region, makes difficult the discrimination of the rate controlling phenomenon, and hence casts a doubt on the value of the rate parameter determined by fitting the model. Criteria such as the effect of particle size are often difficult to apply because of size distribution effects. All these factors have contributed to a lack of precise knowledge of the governing mechanisms and the lack of reliable quantitative information on the kinetics of interfacial polycondensation reactions.

While interpretation of rate data has often been done through models that postulate rate processes in series, ionic equilibria in the aqueous phase have not been considered so far. This can be important, since the water-soluble monomers used in interfacial polycondensations have functional groups (such as $-NH_2$) that often interact with the hydrogen ions in the medium and therefore exist in different forms depending on pH. Available evidence suggests (Bradbury et al., 1968) that it is only the unprotonated form that can take part in the reaction, possibly because of its ability to partition into the site of reaction. Indeed, one of the common methods of quenching the reaction is to lower the pH by acid addition, which suggests that when essentially all the monomer becomes protonated, it becomes unavailable for the reaction.

Characterization of the polymer is usually done through light and/or electron microscopy. In the membrane literature, one finds measurements of pure water permeability and salt rejection. Detailed investigations into the influence of preparation conditions on polymer structure have not been reported.

This work attempts to address some of the lacunae mentioned above. Kinetics of the interfacial polycondensation reaction between a diamine and a diisocyanate have been determined over a range of concentrations using the technique of external pH measurement. The particle-size distribution is kept the same in all the experiments by employing identical conditions of emulsification. The rate of monomer consumption is reduced, by reducing the volume fraction of the dispersed phase (and hence the area available) to a point where it can be measured with confidence. A model is proposed for the reaction that considers ionic equilibria in the external

aqueous phase in addition to the resistances due to external mass transfer, diffusion through the formed polymer and surface reaction. Finally, some studies have been carried out on the crystalline structure of the formed polymer. The observed variations in estimated diffusivities have been rationalized based on the structural information.

Experimental Studies

Materials used

The monomers used in the experiments were Hexamethylene-1,6-Diamine (HMDA) obtained from Merck, Switzerland in $>99\%$ purity, and Hexamethylene-1,6-Diisocyanate (HMDI) obtained from Fluka, Switzerland in $<98\%$ purity. The monomers were used without further purification. Cyclohexane was used as the solvent for the oil-soluble monomer HMDI, and distilled water was used for the water soluble monomer HMDA. Tween-85 (Sigma Chemical Co., USA) was used to stabilize the o/w emulsion in which the reaction was carried out.

Methods

Experiments to produce polyurea microcapsules were conducted using a slight modification of the procedures of Beestman and Deming (1983) and Yadav et al. (1990). In a typical experiment, an emulsion was first prepared by dispersing 50 cm^3 of the organic phase (cyclohexane containing the required number of moles of HMDI) in 100 cm^3 distilled water containing 4 cm^3 of Tween-85. The emulsification was carried out by stirring the two phases for 15 min at 50 rev/s, in a 1,000 cm^3 beaker using a high-speed agitator provided with a shrouded, four-blade pitched turbine (Remi motors Ltd., Model L56-3, with a 1 hp motor). Immediately, the required volume of this emulsion was added to a 250 cm^3 beaker containing the required amount of HMDA dissolved in 100 cm^3 of distilled water, thus initiating the polycondensation reaction between HMDA and HMDI leading to the formation Poly(hexamethylene)urea

$$n\mathrm{H_2N-(CH_2)_6-NH_2} + n\mathrm{OCN-(CH_2)_6-NCO} \rightarrow$$
$$-[\mathrm{HN-(CH_2)_6-NH-OCNH-(CH_2)_6-NHCO}]_n - \quad (1)$$

(In some cases, the emulsion was let stand for up to 10–15 min to see if the hydrolysis of the diisocyanate was significant.) The reaction mixture was kept agitated using a magnetic stirrer. Since HMDA solution is alkaline, consumption of HMDA by reaction was monitored by following the pH of the aqueous phase continuously with time using a pH probe. When the pH attained a constant value, indicating completion of the reaction, the agitation was stopped and the microcapsules were filtered out. The time constant of the probe was checked by letting the response become steady in a buffer solution, abruptly shifting the probe to a solution of a different pH and noting the time required for completion of the response. The response was complete in 1.5–2.5 s, the shorter response times obtaining for freshly cleaned probes.

Samples of the polymer for structural studies were prepared by grinding the capsules using a mortar and pestle, washing out the adhering reactants and solutions and drying the polymer. Powder X-ray diffraction (XRD) patterns of the polymer samples were recorded in the reflection mode on a wide angle X-ray (WAXS) diffractometer using a Rigaku goniometer (RIGAKU-DMAX/1C). Ni-filtered Cu-Kα radiation from a 20 kV, 40 mA rotating anode source was used.

All experiments were conducted in duplicate using the same emulsion. The pH values at different times used in the data interpretation were the averages of the observations in the two runs. In some cases, the entire run was repeated including the emulsification step in order to check the reproducibility of the pH-time data.

Calibrations of pH as a function of the concentration of HMDA in the range of interest were prepared using standard solutions of known HMDA concentrations using emulsions of the kind used in the actual experiments, but prepared without the HMDI to avoid reaction. Both types of calibrations were repeated periodically. While these showed minor variations, it was found that on logarithmic coordinates they were essentially parallel to each other and to the theoretically predicted curve for pure HMDA-water system (Yadav et al., 1990). A typical set of such calibration data is shown in Figure 1. The data are fitted well by an equation of the form

$$C_T = \hat{A}h^{-p} \quad (2)$$

where C_T is the concentration of the HMDA (kmol·m^{-3}), h is the hydrogen ion concentration, and $\hat{A}$ and p are constants fitted from the calibration plot. The differences in calibrations mentioned above thus showed up as small variations in the value of $\hat{A}$ and could be accounted for by normalizing the pH data with respect to the initial pH obtained in the experiments (for which the concentration of HMDA was known).

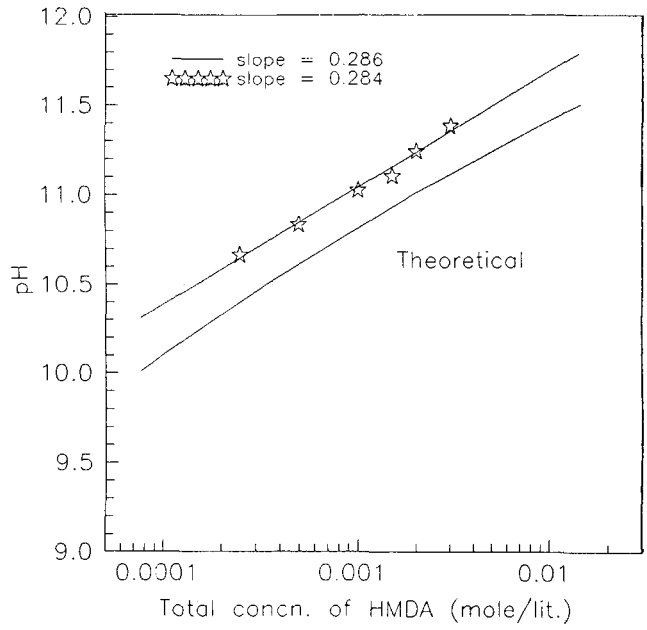

Figure 1. Calibration plots of pH vs. concentration of HMDA (C_T).

Theoretical calibration is also shown.

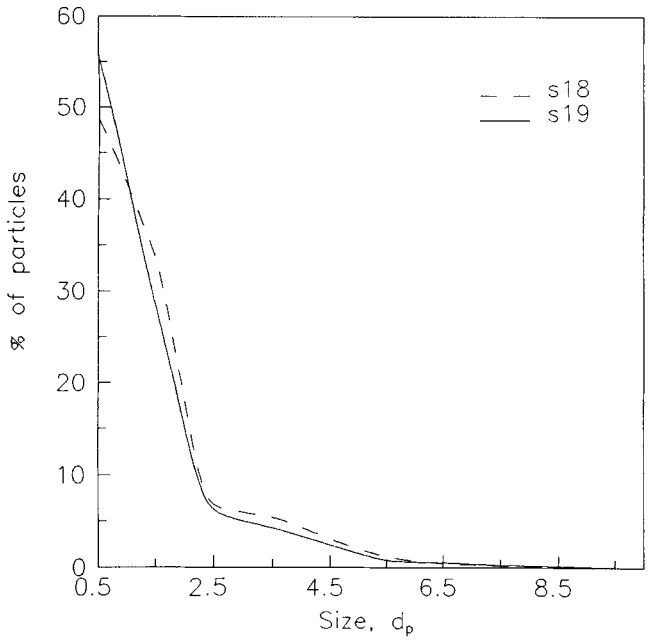

Figure 2. Typical size distribution of capsules, as measured for two cases.

All reactions were carried out at the ambient temperature of 27° – 28°C. The capsule sizes were kept the same in all the experiments by always using the same conditions for emulsification. The volume of this emulsion used subsequently determined the phase volume ratio during the reaction, and hence the area available. Apart from phase volume ratio, the effect of monomer mole ratio (ratio of HMDI to HMDA R varied between 0.8 and 5) and the number of moles of the limiting monomer (n_L) (kmol) on the kinetics was studied. The concentrations of HMDA that resulted were such that a reasonable variation in pH would be expected over the conversion range of interest.

The size distribution of capsules was determined in a particle-size analyzer Galai CIS-1. The Galai CIS-1 is a laser based system that combines the time of transition theory and advanced image analysis for particle analysis and image verification. A typical size distribution is shown in Figure 2. The size range of the microcapsules was typically 0.5–10 μm and the mean diameter of the capsules was 1.6 μm.

Theoretical

Assumptions

For purposes of modeling, it is assumed that the organic phase containing monomer A (HMDI) is dispersed in the form of identical drops (of diameter d_p) (m) in the aqueous phase. Only differences from previous work are described below. Refer to Yadav et al. (1990) for other details. The transport processes considered are the mass transfer in the external phase, diffusion through the polymer layer, and interfacial reaction operating in series. The mass-transfer coefficient in the continuous phase considering the small size of the particles may be calculated assuming a Sherwood number of 2. It is assumed that only the unprotonated form of hydrophilic monomer B (HMDA) can partition into and diffuse through the polymer phase, and hence participate in the reaction with A.

Ionic equilibria in continuous phase

The fraction of monomer B in the aqueous phase that is unprotonated depends on the pH, which varies through the run, decreasing as the concentration of A decreases due to reaction. The following ionic equilibria operate in the continuous phase.

$$H_3^+N-R-NH_3^+ \rightleftharpoons H_3^+N-R-NH_2+H^+ \quad (3)$$

$$H_3^+N-R-NH_2 \rightleftharpoons H_2N-R-NH_2+H^+ \quad (4)$$

In the bulk aqueous phase, the concentration of the unprotonated form of the diamine C_{Bb} (kmol·m^{-3}) may be related to the total concentration C_T of all three forms using the ionic equilibrium conditions

$$C_{Bb}=\frac{C_T}{1+\frac{h}{K_{a2}}+\frac{h^2}{K_{a1}K_{a2}}} \quad (5)$$

where h is the hydrogen ion concentration and K_{a1} and K_{a2} are respectively the equilibrium constants of reactions 4 and 3 above.

Concentration profile of HMDA in film

Figure 3 shows the processes assumed to be taking place and the resulting concentration profiles. In microencapsulation, the wall thickness is usually much smaller than the capsule radius. Neglecting curvature therefore and using carte-

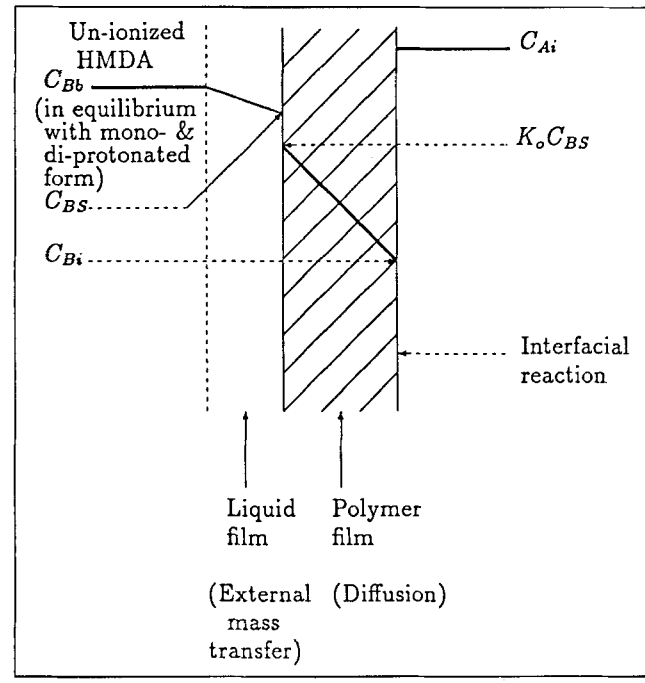

Figure 3. Concentration profiles resulting from the rate and equilibrium processes.

sian co-ordinates, the diffusion of B through the polymer layer under quasi-steady-state conditions is described by the following equation, where C_B is the concentration of HMDA ($kmol \cdot m^{-3}$) at a distance x from the aqueous phase-polymer interface

$$D_B \frac{d^2 C_B}{dx^2} = 0 \tag{6}$$

with

$$C_B = K_0 C_{Bs} \qquad \text{at } x = 0$$
$$C_B = C_{Bi} \qquad \text{at } x = \delta$$

A flux balance at the reaction surface gives

$$- D_B \left. \frac{dC_B}{dx} \right|_i = k' C_{Bi} C_{Ai} \tag{7}$$

where k' is the surface reaction rate constant ($m^4 \cdot kmol^{-1} \cdot s^{-1}$).

In terms of the following nondimensional variables

$$Y_B = \frac{C_B}{K_0 C_{B0}}, \qquad Y_{Bs} = \frac{C_{Bs}}{C_{B0}}, \qquad Y_{Bi} = \frac{C_{Bi}}{K_0 C_{B0}},$$
$$Y_{Ai} = \frac{C_{Ai}}{C_{A0}}, \qquad \zeta = \frac{x}{\delta_f}$$

(where δ_f is the final microcapsule shell thickness, m), the above equations can be solved to give

$$Y_B = - \left(\frac{\phi Y_{Ai} Y_{Bs}}{1 + \phi Y_{Ai} \zeta_t} \right) \zeta + Y_{Bs} \tag{8}$$

where

$$\phi = k' \delta_f C_{A0} / D_B$$

Progress of reaction in time

We define a bulk conversion X of the monomer B, which can be related to the pH of the medium through Eq. 1, as

$$X = 1 - (C_T / C_{T0}) = 1 - H^{-p} \tag{9}$$

where $H = h/h_0$ is the nondimensionalized hydrogen ion concentration, nondimensionalized with respect to the initial value h_0. Neglecting the small holdup of the monomer B in the polymer film and the changes in the volumes of the bulk phases, the time varying bulk concentrations and the film thickness may be related to each other and to conversion using the stoichiometry of the reaction

$$\left(\frac{6 V_d \rho_p}{d_p \alpha} \right) \delta = M V_c C_{T0} X = M V_d (C_{A0} - C_A) \tag{10}$$

where α is the volumetric swelling factor, defined as the ratio between the volumes of the swollen and unswollen polymer, and M is the sum of the molecular weights of the two monomers ($kg \cdot kmol^{-1}$).

If R is the initial mole ratio of monomer A to monomer B and n_L is the number of moles of the stoichiometrically limiting monomer (i.e., moles of HMDA if $R > 1$ and moles of HMDI if $R < 1$), we have the above in the following nondimensional forms

$$\zeta_t = \frac{V_c C_{T0} X}{n_L} = aX \tag{11}$$

$$Y_{Ai} = \frac{R - X}{R} \tag{12}$$

where the constant $a = 1$ if $R > 1$, and $a = 1/R$ if $R < 1$. Equating the rate of change of HMDA concentration in the external phase to the rate of external mass transfer and in turn to the rate of uptake by the forming capsules $\Re$, we have

$$- V_c \frac{dC_T}{dt} = k_L \hat{a} V_c (C_{Bb} - C_{Bs}) = \Re V_c \tag{13}$$

where

$$\Re = - \frac{6 V_d}{d_p V_c} D_B \left. \frac{dC_B}{dx} \right|_{x=0}$$

In terms of the following nondimensional variables

$$Y_T = C_T / C_{B0}, \qquad Y_{Bb} = C_{Bb} / C_{B0}$$

Eq. 13 becomes

$$- \frac{dY_T}{dt} = k_L \hat{a} (Y_{Bb} - Y_{Bs}) = \frac{\Re_{\max}}{C_{B0}} \left(\frac{Y_{Ai} Y_{Bs}}{1 + \phi Y_{Ai} \zeta_t} \right) \tag{14}$$

In the above, Y_T refers to the total concentration of the three forms of monomer B in the continuous phase, while Y_B refers only to the unprotonated form. Further,

$$\Re_{\max} = \frac{6 V_d}{d_p V_c} (k' K_0 C_{B0} C_{A0}) \tag{15}$$

is the maximum possible rate of reaction in moles per unit time per unit volume of the continuous phase.

Eliminating Y_{Bs}, putting $\phi_e = \Re_{\max} / (k_L \hat{a} C_{B0})$ and rearranging

$$- \frac{dY_T}{dt} = k_L \hat{a} Y_{Bb} \left(\frac{\phi_e Y_{Ai}}{1 + \phi Y_{Ai} \zeta_t + \phi_e Y_{Ai}} \right) \tag{16}$$

Variation of external phase pH with time

Using the Eqs. 9–12, Eq. 16 can be expressed in terms of conversion. It is preferable however to have the equations

directly in terms of the measured variable, the hydrogen-ion concentration. Using Eq. 5, we have

$$Y_T = \frac{C_T}{CB_0} = \frac{h^{-p}}{h_0^{-p}}\left(1 + \frac{h}{K_{a2}} + \frac{h^2}{K_{a1}K_{a2}}\right) \tag{17}$$

Substituting for all the variables in Eq. 16 in terms of H, we get

$$\frac{dH}{dt} = \left[\frac{(\Re_{\max}/pC_{B0})\,[1/(1/H + K_1 + K_2H)]}{\phi_e + a\phi(1 - H^{-p}) + R/[R - (1 - H^{-p})]}\right] \tag{18}$$

where the constant $K_1 = h_0/K_{a2}$ and $K_2 = h_0^2/(K_{a1}K_{a2})$.

On integrating Eq. 18 with the initial condition of $H = 1$, we get

$$t = \frac{p}{k_L\hat{a}}\left[\ln H + K_1(H-1) + \frac{K_2}{2}(H^2-1)\right]$$
$$+ p\left(\frac{d_pV_c}{6V_d}\right)^2\left(\frac{\alpha MC_{T0}}{\rho_pK_0D_B}\right)\left[\ln H + K_1(H-1) + \frac{K_2}{2}(H^2-1)\right.$$
$$\left. + \frac{H^{-p}-1}{p} + \frac{K_1}{p-1}(H^{-p+1}-1) - \frac{K_2}{2-p}(H^{2-p}-1)\right]$$
$$+ \frac{pd_pK_i}{6k'K_0C_{T0}}\left[\frac{1}{(R-1)p}\ln\left(\frac{(R-1)H^p+1}{R}\right)\right.$$
$$+ K_1\int_1^H\left(\frac{H^p}{(R-1)H^p+1}\right)dH$$
$$\left. + K_2\int_1^H\left(\frac{H^{p+1}}{(R-1)H^p+1}\right)dH\right] \tag{19}$$

Analysis of rate expression

In the above development, the parameter ϕ_e (external mass-transfer term) compares a characteristic reaction rate to a characteristic external mass-transfer rate, while ϕ compares in a similar manner a reaction rate with a diffusion rate through the polymer film. While the magnitudes of these parameters can therefore be used to judge which rate phenomenon controls (if any) in a given situation, it is quite possible for the controlling regime to change during the reaction. Thus, the diffusion resistance is obviously nonexistent at the start (there being no film) and increases in importance as the film grows in thickness. The three terms in the denominator of Eq. 18 compare these resistances at any point in time. The time required for a given conversion in Eq. 19 may also be interpreted in similar fashion, as the sum of the contributions due to external transport, and diffusion through polymer and interfacial reaction. Under conditions of kinetic control, omitting the terms in Eq. 19 which are not relevant, we get a function $f_k(H)$, which will plot linearly with time, as follows

$$f_k(H) = \left[\frac{1}{(R-1)p}\ln\left(\frac{(R-1)H^p+1}{R}\right)\right.$$
$$+ K_1\int_1^H\left(\frac{H^p}{(R-1)H^p+1}\right)dH$$
$$\left. + K_2\int_1^H\left(\frac{H^{p+1}}{(R-1)H^p+1}\right)dH\right] \tag{20}$$

Similarly, under conditions of diffusion control, we have a linear relation between $f_D(H)$ and time, where

$$f_D(H) = \left[\ln H + K_1(H-1) + \frac{K_2}{2}(H^2-1)\right.$$
$$\left. + \frac{H^{-p}-1}{p} + \frac{K_1}{p-1}(H^{-p+1}-1) - \frac{K_2}{2-P}(H^{2-p}-1)\right] \tag{21}$$

Results and Discussion

General observations

Table 1 shows the conditions employed in the kinetic studies. The nominal shell thickness denotes the thickness of the dry polymer layer as calculated by stoichiometry (Eq. 10) at complete conversion. Some general observations on the results of the experiments are in order. Initially, two volume ratios (V_d/V_c) were used: 0.25 and 0.045. It was found that, in the former case (concentrated emulsion), the pH dropped very fast because of the large interfacial area available for the reaction. Therefore, experiments for the estimation of kinetic parameters were carried out with the dilute emulsion ($V_d/V_c = 0.045$) and only these are shown in Table 1. Even here, rates at the mole ratio of 5 were often fast and not always useful for parameter estimation. It was observed that a certain minimum number of moles of the limiting monomer was necessary in order to form a coherent and self-supporting film. If n_L was too small, no capsules were found when the reaction mixture was filtered at the end, indicating that either no film was formed, or the film was too thin to hold together and broke immediately. This was observed in our experiments whenever the number of moles of the limiting monomer per unit interface was smaller than 5.33×10^{-9}

Table 1. Conditions Used in Kinetic Studies

V_d/V_c	Limiting Monomer $n_L \times 10^4$ mol	Bulk Mole Ratio, R = HMDI/HMDA							Nominal Shell Thickness
		5.0	1.563	1.25	1.1	1.0	0.9	0.8	μm
0.045	24.0			s43					0.036
0.045	6.0	s29		s18 s19	s26	s31 s44 s53		s34	0.0092
0.045	3.0	s14	s20	s33	s27	s15			0.0046
0.045	2.4						s24		0.0037
0.045	1.0	s30		s21	s28	s32		s36	0.0015
0.045	0.9						s25		0.0014

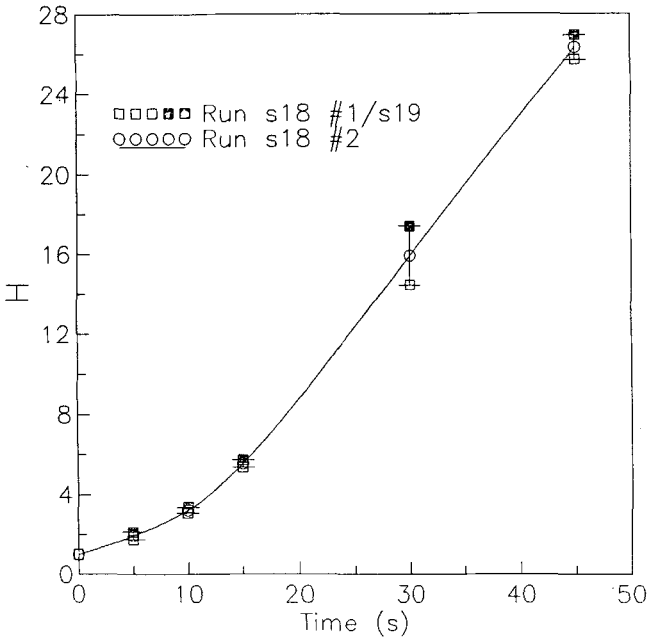

Figure 4. Variation of dimensionless H-ion concentration with time (runs s18 and s19).

$V_d/V_c = 0.045$; $R = 1.25$; $n_L = 6 \times 10^{-4}$ mol.

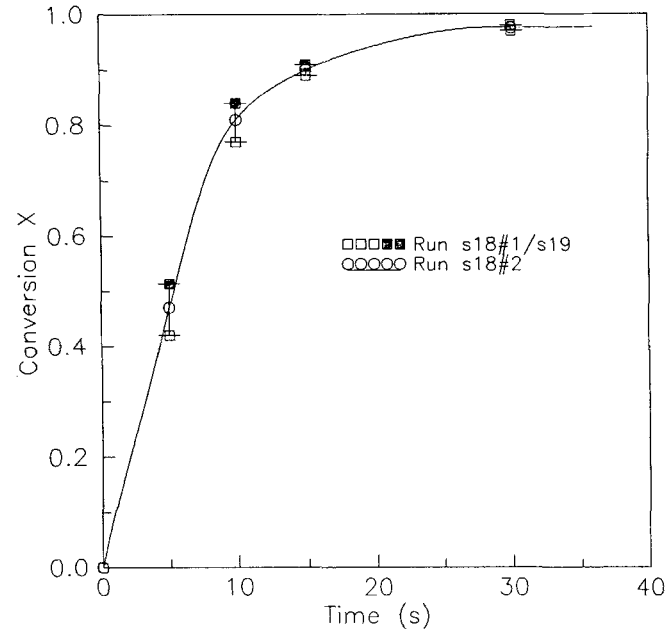

Figure 5. Conversion-time data for runs s18 and s19.

$V_d/V_c = 0.045$; $R = 1.25$; $n_L = 6 \times 10^{-4}$ mol.

kmol/m^2 (last two rows of Table 1). The diffusion resistance in such experiments would therefore be expected to be quite small and estimates of the reaction rate constant would be reliable.

Validation of experimental technique

Figure 4 shows the pH (plotted as the dimensionless hydrogen ion concentration H) vs. time data for experiments in a dilute emulsion with a mole ratio R of 1.25 (Runs S18 and S19 in Table 1). The experimental points refer to three experiments carried out with the same conditions in order to check the reproducibility of the experiments. Two of these experiments (s18, runs #1 & #2) were carried out one after the other, using different aliquots of the same emulsion (prepared in a sufficient amount to last for several runs), and the third experiment (s19) was a repetition from the start, including the emulsion preparation step. It is seen that the reproducibility of the data is satisfactory, demonstrating the reliability of the method used in the kinetic measurements. The isocyanate groups (in HMDI) have a tendency to hydrolyze and produce amino groups. The good correspondence between the first two runs shows that on the timescale of the experiment the extent of hydrolysis of the diisocyanate is negligible. For, if significant hydrolysis had occurred by the time run 2 was carried out, the rate in the second experiment would have been lower because of (a) a reduced HMDI concentration, and (b) the possibility of a polyurea film having been formed by the reaction between HMDI and its hydrolysis product. Bradbury et al. (1968) obtained a similar result to ours in their experiments. The good agreement between the runs repeated in their entirety (s18 and s19) show satisfactory reproducibility of all the process steps including emulsification. The same data on conversion-time coordinates in Figure 5 confirms the reproducibility, and also shows that the rates are slowed down sufficiently in the dilute emulsion system where data over a range of conversion can be obtained for estimation of rate parameters.

Regimes of reaction

A conservative calculation of the external mass-transfer rate (assuming a Sherwood number of 2) and its comparison with the observed rates of reaction shows that external mass-transfer resistance is quite small in general for the particle sizes and concentrations used. The discussion in this section will therefore be concerned with the resistances due to diffusion and interfacial reaction.

While one way to establish the operating regime would be to make appropriate plots as described in a previous section (Eqs. 20 and 21) and examine their linearity, it would be more conclusive to do this directly from the data, not invoking the model to the extent possible. The effect of the concentrations of the monomers on the rate of the reaction can give useful pointers to the relative importance of diffusional and kinetic factors. If the reaction were kinetically controlled, the observed rate would be proportional to the product of the concentrations of the two monomers. On the other hand, if the reaction were diffusion controlled, the rate would be directly proportional to C_{B0} and inversely proportional to the film thickness (and hence $C_{T0}X$, see Eq. 10). Consider experiments with the same initial mole ratio of the monomers but different number of moles of the limiting monomer, i.e., experiments along a column of Table 1. The foregoing analysis shows that, if the rates were to be compared at equal conversions, they would scale as the product of the initial concentrations if kinetic control prevails, and be nearly equal if diffusion control prevails. The variation of pH does introduce some complication since it makes part of the diamine in the external phase unavailable for reaction. It may be shown that,

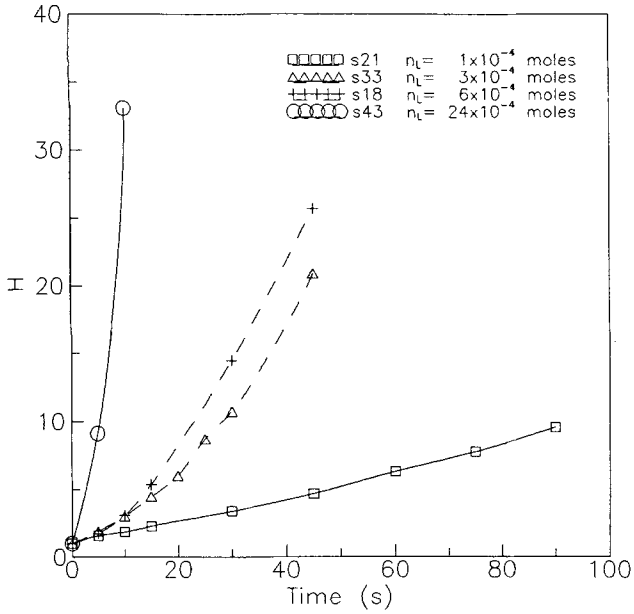

Figure 6. H vs. time for experiments with the same R ($R = 1.25$) but different n_L.

It shows the dominant influence of kinetic resistance.

if this were to be considered, the ratio of the rates for the two cases should increase from its value initially as conversion increases, for both kinetic control as well as diffusion control.

Figure 6 compares the data from four such experiments at $R = 1.25$ with different values of n_L. The figure shows that the rates are significantly different in all cases, showing that kinetic factors are important over at least a substantial part of the conversion range. The average rates to different values of H, in these experiments and in similar sets $R = 1.1$ and 1.0, are tabulated in Tables 2–4 respectively. Average rates (calculated by dividing the number of moles of diamine converted by the time elapsed) are used since the accuracy and spacing of data does not warrant calculation of instantaneous rates by differentiation. The rates tabulated are values relative to those in the base case (identified in the table), and are to be compared with relative values of the products of initial concentrations (shown at the top of each column). It is seen in all cases that the relative rates do vary with the product of initial concentrations, and scale approximately as their product. Thus, diffusional control over a substantial part of the experiment can be ruled out, although a mixed control towards the end of the experiments remains a possibility.

Table 3. Relative Average Rates at Different Conversions for Experiments with Mole Ratio $R = 1.1$

Sample Code →	s28*	s27	s26
$(C_{T0}\,C_{A0}/(C_{T0}\,C_{A0})^*$ →	1	9	36
H ↓	Relative Rates ↓		
2.5	1	6.24	26.24
5.0	1	6.74	31.92
7.5	1	7.03	33.30
10.0	1	7.8	37.95
12.5	1	8.36	41.61

*The base case, relative to which data from other runs are reported.

Parameter estimates

The foregoing discussion shows that, kinetic resistance being the more important, it is the reaction rate constant k' that can be estimated more accurately than the diffusivity D_B from the experimental data. Further, the diffusional resistance will be the less important, the lesser the film thickness, and the best estimates of k' are probably to be obtained from the experiments in the last two rows of Table 1. Figure 7 shows plots of the function $f_k(H)$ vs. time for these experiments, in which n_L was too small for a self-supporting film to form. The rates in these experiments were sufficiently slow that data over a sufficiently wide range of conversions could be obtained. The data plot reasonably linearly in all cases until conversions of about 75%. The rate constant of the interfacial reaction can be calculated from the slopes of the best-fit lines. The values so obtained are shown in Table 5 where the 95% confidence limits are also shown. The values of k' were further refined by fitting the data to Eq. 19 by a nonlinear regression procedure, taking the above values as initial estimates. For this purpose, the experimental pH values were converted to H and used as the dependent variable. Since Eq. 19 is explicit in time, the Ridder's algorithm (Press et al., 1993) was used to invert this relationship and calculate H as a function of time. The integrals in Eq. 19 were numerically evaluated using an implementation of Simpson's rule (Press et al., 1993). The sum of squares of relative error in H was minimized using a multivariable Golden Search method. The values of k' thus estimated are also shown in Table 5. The sum of squares of relative error between predicted and measured conversion has also been reported for each case.

Table 2. Relative Average Rates at Different Conversions for Experiments with Mole Ratio $R = 1.25$

Sample Code →	s21	s33*	s18	s43
$(C_{T0}C_{A0}/C_{T0}\,C_{A0})^*$ →	0.11	1	4	64
H ↓	Relative Rates ↓			
5	0.110	1	2.24	45.73
7.5	0.100	1	2.42	41.95
10	0.102	1	2.48	46.50
15	—	1	2.39	42.80
20	—	1	2.32	43.50

*The base case, relative to which data from other runs are reported.

Table 4. Relative Average Rates at Different Conversions for Experiments with Mole Ratio $R = 1.0$

Sample Code →	s32*	s15	s53
$(C_{T0}\,C_{A0})/(C_{T0}\,C_{A0})^*$ →	1	9	36
H ↓	Relative Rates ↓		
2.5	1	6.00	20.05
5.0	1	6.93	25.80
7.5	1	7.51	27.18
10.0	1	7.45	23.64
12.5	1	10.19	24.77

*The base case, relative to which data from other runs are reported.

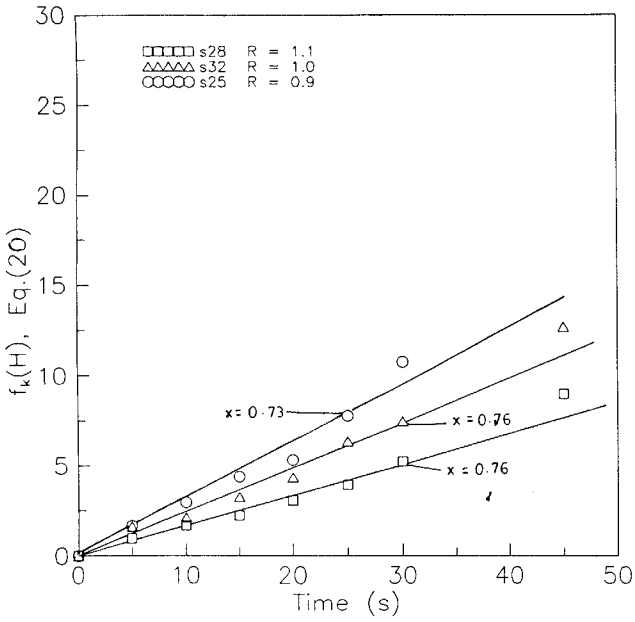

Figure 7. Linearity of f_k(H) vs. time for case of $n_L = 1 \times 10^{-4}$ mol.

The conversion marked on the curves are the values till which linearity holds.

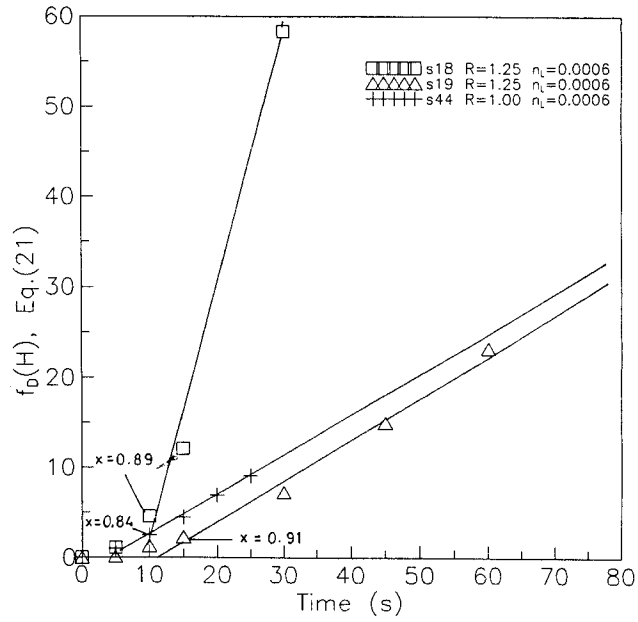

Figure 8. High conversion data showing possible diffusion control.

Conversion marked are the values beyond which f_D(H) vs. time data are linear.

The rate constant is of order 10^{-7} m^4/(kmol·s), which agrees with the values reported in previous work with Butachlor (Yadav et al., 1990). While there is some scatter, the average value is about 2.6×10^{-7} m^4/kmol/s.

While it is unlikely that accurate values of D_B can be obtained from these data, an attempt was made to estimate it at least approximately. As Figure 8 shows, the high conversion data ($X > 0.85$) in experiments to form thicker films often showed reasonable linearity when plotted as $f_D(H)$ vs. time. Estimates of D_B from the slopes of such plots were refined by nonlinear regression as explained earlier, using the value of k' already estimated as a known constant. This was done to avoid the problem of correlation of parameters that was sometimes experienced when a two parameter search was attempted. The values of D_B obtained are shown in Table 6. While they show considerable scatter, the values are generally in the range $10^{-13} - 10^{-14}$ m^2/s. It may be noted that the higher values of diffusivity tend to correlate with the formation of thicker films. In general, diffusivity would depend on the structure of the film formed and could therefore vary from experiment to experiment. Indeed, variations are possible even within the same experiment as the nature of the polymer precipitated could vary with time, and a constant diffusivity approach such as the one used in this article is an approximation that gives average values. The fit of the model (with the average value from Table 5 for k' and D_B as estimated) is shown in Figures 9 and 10.

Correlation between rate and structure

The foregoing discussion relating to the values of diffusivity obtained suggest that the polymer films formed under different conditions could possess differences in structure leading to differences in diffusivity. This would be clearly of relevance in microencapsulation because of its implications on release rates from the capsules produced. As shown, the higher diffusivities obtained were in the case of thicker films in order to form which higher concentration of monomers

Table 5. Value of Interfacial Reaction Rate Constant k'

				$k' \times 10^7$ m^4/(kmol·s)			
				Estimated from Figure 7			
Run No.	$n_L \times 10^4$ mol	R	δ_f μm	Parameter Value	95% Confidence Limits	Est. From Eq. 19	Sum of Squares of Residuals
s21	1.0	1.25	0.0015	2.32	$2.28 \le k' \le 2.36$	1.89	0.027
s28	1.0	1.10	0.0015	1.97	$1.94 \le k' \le 2.00$	2.15	0.059
s32	1.0	1.00	0.0015	2.55	$2.51 \le k' \le 2.59$	3.14	0.035
s36	1.0	0.80	0.0015	2.00	$1.93 \le k' \le 2.07$	2.05	0.021
s25	0.9	0.90	0.0014	3.41	$3.34 \le k' \le 3.48$	3.73	0.045

Table 6. Value of Diffusivity D_B obtained by Fitting Data to Eq. 19

Run No.	$n_L \times 10^4$ mol.	R	δ_f μm	$D_B \times 10^{14}$ m^2/s Estimated from Figure 8 Parameter Value	95% Confidence Limits	Est. From Eq. 19	Sum of Squares of Residuals
s18	6.0	1.25	0.0092	98.50	$97.05 \le D_B \le 99.95$	63.10	0.100
s19	6.0	1.25	0.0092	12.40	$12.34 \le D_B \le 12.46$	10.00	0.102
s26	6.0	1.25	0.0092	7.17	$7.11 \le D_B \le 7.23$	10.00	0.022
s53	6.0	1.25	0.0092	7.99	$7.97 \le D_B \le 8.01$	26.20	0.042
s20	3.0	1.56	0.0046	4.40	$4.35 \le D_B \le 4.45$	3.21	0.058
s33	3.0	1.25	0.0046	6.00	$5.88 \le D_B \le 6.12$	8.41	0.061
s24	2.4	0.90	0.0037	0.77	$0.76 \le D_B \le 0.78$	1.53	0.023

had been used. The rate of polymerization for these cases would be therefore higher on the average than in the case of thinner films. The possibility was considered that the polymer film formed under conditions of high rates of polymerization tended to have a high amorphous content, since amorphous polymers show higher diffusivities than crystalline polymers.

Figures 11 and 12 show the powder XRD patterns for two of the polymer samples, s29 and s15. The conditions for preparation were such that the initial rates for s29 would be about twenty times that for s15. While both samples are seen to be semicrystalline, the XRD patterns clearly show that s29 is more amorphous than s15. An amorphous halo drawn on these diagrams, as shown in Figures 11 and 12, allows calculation of a degree of crystallinity in each case by comparing the area under the crystalline peaks and the total area. Such calculations show the degree of crystallinity of s29 to be 21.3% and s15 to be 44.5%. It is likely that, when polymer molecules form and precipitate out at high rates, they do not get sufficient time to arrange themselves in an ordered lattice. It seems thus possible to vary the structure and hence the diffusivity of these polymer films through the conditions employed in their preparation. More work on the development of clear correlations between preparation conditions, polymer crystallinity, and release rates thus seems worthwhile.

Conclusions

Kinetic data on the interfacial polycondensation reaction between HMDI and HMDA, in the encapsulation of cyclohexane, have been obtained over a range of concentrations and film thicknesses using the measurement of pH variation during reaction. The reaction velocity has been reduced to a point where it can be measured reasonably accurately by reducing the area available for reaction, keeping the size distribution of the capsules the same. It has been found that the

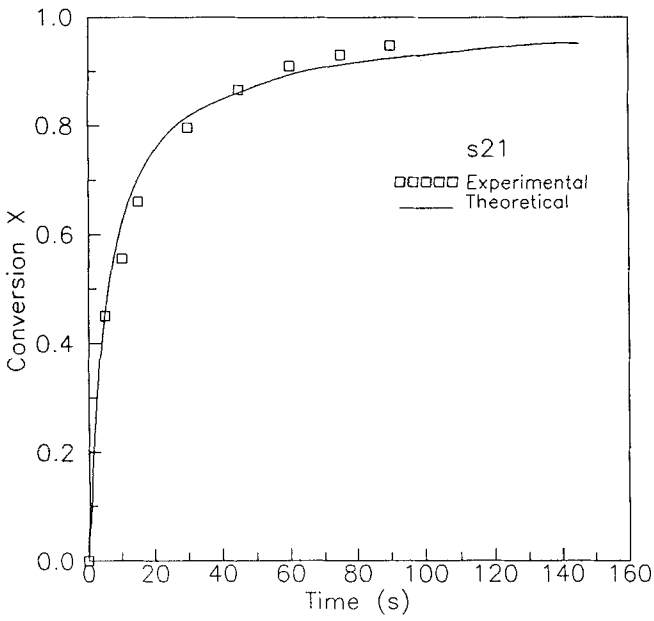

Figure 9. Fit of the model to experimental data with fitted values of the rate parameters.
$R = 1.25$; $n_L = 1 \times 10^{-4}$.

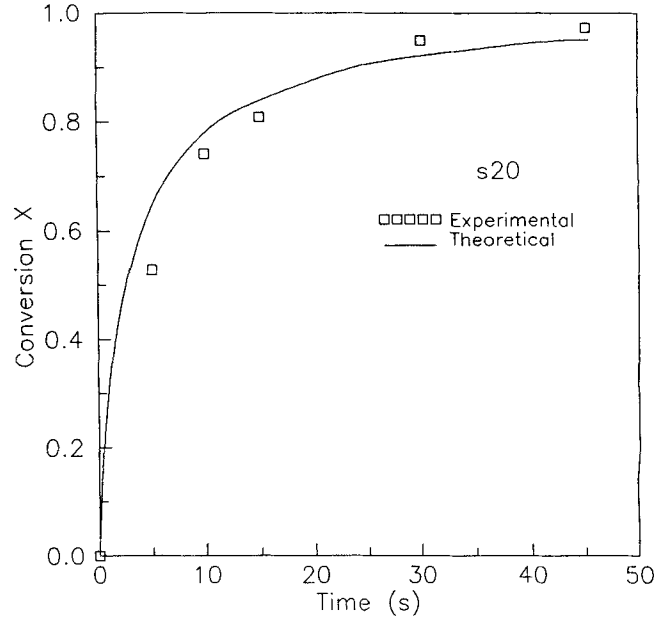

Figure 10. Fit of the model to experimental data with fitted values of the rate parameters.
$R = 1.56$; $n_L = 3 \times 10^{-4}$.

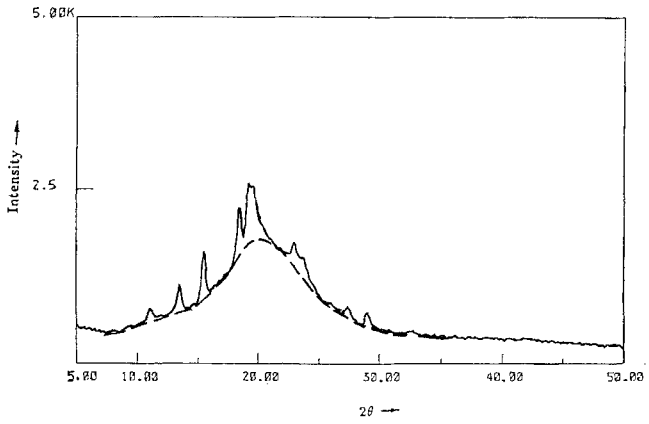

Figure 11. XRD pattern for Polyurea sample s29.

$V_d/V_c = 0.045$; $R = 5.0$; $n_L = 6 \times 10^{-4}$, mol. The dashed line shows the amorphous halo drawn for the purpose of calculating degree of crystallinity.

reaction proceeds under kinetic control over at least a substantial part of the conversion range. It has also been observed that no self-supporting film forms if the number of moles of limiting monomer is too small, since the amount of polymer formed would be too small. In our experiments, no capsules could be recovered if the number of moles of limiting monomer per unit interfacial area was less than 5.33×10^{-9} kmol/m^2.

A theoretical model for the kinetics has been developed that considers ionic equilibria in the external phase, and the rate processes of external mass transfer, diffusion through the formed polymer and interfacial reaction as operating in series. The model has been shown to fit the data well. The regressed values of the reaction rate constant and diffusivity agree in their orders of magnitude with the values available in literature for similar systems.

Comparison of the XRD patterns obtained from polymers formed under conditions of high and low rates show that the polymer formed at high rates is more amorphous. This is likely because of time constraints that exist for crystallization when polymer molecules precipitate out at a high rate. Such differences in the structure of the polymer as formed are important since the diffusivity of the encapsulated species through the polymer, and hence the release rate, depends on the structure.

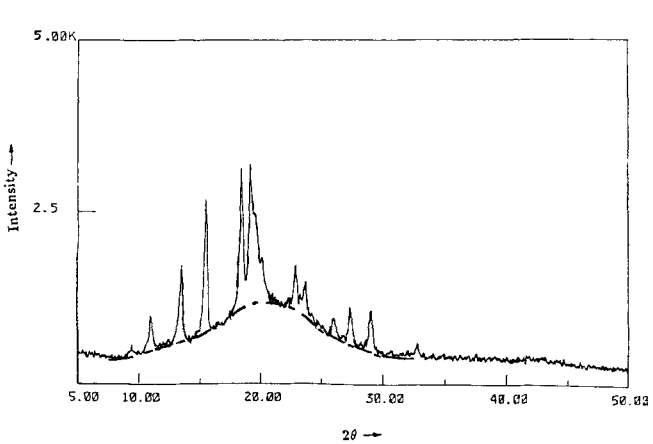

Figure 12. XRD pattern for Polyurea sample s15.

$V_d/V_c = 0.045$; $R = 1.0$; $n_L = 3 \times 10^{-4}$ mol. The dashed line shows the amorphous halo drawn for the purpose of calculating degree of crystallinity.

Notation

$\hat{a}$ = interfacial area per unit vol. of continuous phase
C = concentration of cyclohexane in *n*-Heptane, kmol·m^{-3}
C_{Ai} = concentration of monomer A in the core liquid at any time, kmol·m^{-3}
C_{A0} = initial concentration of monomer A in the liquid core, kmol·m^{-3}
C_{Bi} = concentration of monomer B at the inner radius of the shell, kmol·m^{-3}
C_{B0} = initial concentration of monomer B (unprotonated form) in the bulk phase, kmol·m^{-3}
C_{Bs} = concentration of monomer B at the outer surface of the polymer shell, kmol·m^{-3}
D_B = effective diffusivity of monomer B, m^2·s^{-1}
K_i = partition coefficient of monomer B between polymer and organic phase
k_L = external mass-transfer coefficient for monomer B, m·s^{-1}
K_0 = partition coefficient of monomer B between aqueous and polymer phase
Y_{Ai} = nondimensional concentration of monomer A in the core liquid at any time
Y_{Bb} = nondimensional concentration of monomer B (unprotonated form) in the bulk phase
Y_{Bi} = nondimensional concentration of monomer B at the reaction zone
ρ_p = density of polyurea formed, kg·m^{-3}

Literature Cited

Beestman, G. B., and J. M. Deming, "Encapsulation by Interfacial Polycondensation," U.S. Patent No. 4,417,916 (1983).

Bradbury, J. H., P. J. Crawford, and A. N. Hambly, "Kinetics of an Interfacial Polycondensation Reaction Part 2.—Reaction of Terephthaloyl Chloride and Piperazine," *Trans. Faraday Soc.*, **65**, 1337 (1968).

Chai, G. Y., and W. B. Krantz, "Formation and Characterization of Polyamide Membranes via Interfacial Polymerization," *J. Memb. Sci.*, **93**, 175 (1994).

Chang, T. M. S., "Semipermeable Microcapsules," *Science*, **146**, 524 (1964).

Janssen, L. J. J. M., and K.te Nijenhuis, "Encapsulation by Interfacial Polycondensation. I. The Capsule Production and a Model for Wall Growth," *J. Memb. Sci.*, **65**, 59 (1992).

Koestler, R. C., *Microcapsulation Using Interfacial Polymerisation Techniques—Agriculatural Application in Controlled Release Technology*, Vol. II, A. F. Kydoniens, ed., CRC Press, Boca Raton, FL, p. 117 (1980).

Kondo, T., *Microcapsules: Their Preparation and Properties in Surface and Colloid Science*, Vol. 10, E. Matijevic, ed., Plenum Press, New York (1978).

MacRitchie, F., "Mechanism of Interfacial Polymerization," *Trans. Faraday Soc.*, **65**, 2503 (1968).

Morgan, P. W., *Condensation Polymers by Interfacial and Solution Methods*, Interscience, New York (1965).

Pearson, R. G., and E. L. Williams, "Interfacial Polymerization of an Isocyanate and a Diol," *J. Poly. Sci.*, Polymer Chemistry Ed., **23**, 9 (1985).

Press, W. H., S. A. Teukolsky, W. T. Vellerling, and B. P. Flannery, *Numerical Recipes in FORTRAN—The Art of Scientific Computing*, 2nd ed., Cambridge Univ. Press (1993).

Sirdesai, M., and K. C. Khilar, "A Model for Microencapsulation in Polyurea Shell by Means of Interfacial Polycondensation," *Can. J. Chem. Eng.*, **66**, 509 (1988).

Yadav, S. K., A. K. Suresh, and K. C. Khilar, "Microencapsulation in Polyurea Shell by Interfacial Polycondensation," *AIChE J.*, **36**, 431 (1990).

Manuscript received May 3, 1995, and revision received Feb. 20, 1996.